# MODELLING ULTRASOUND CONTRAST AGENTS: CURRENT CHALLENGES

E Stride Dept. Mechanical Engineering, University College London, London, UK
M Tang Dep. Bioengineering, Imperial College London, London, UK
R Eckersley Dept. Imaging Sciences, Imperial College London, London, UK

## 1 INTRODUCTION

Microbubbles stabilized by a surfactant or polymer coating have become established as the most effective form of contrast agent available for ultrasound imaging. Due to their high compressibility, they are able to scatter ultrasound far more efficiently than red blood cells. Moreover, at moderate excitation pressures they exhibit a non-linear response which enables their scattered signal to be clearly distinguished from that due to tissue. They thus provide an excellent means of imaging tissue perfusion, particularly for cardiovascular applications and cancer diagnosis[1]. In addition to their use in diagnostic imaging, microbubbles have also shown great promise in therapeutic applications such as targeted drug delivery and gene therapy[2]. Drugs or DNA can be incorporated into the microbubble coating, traced through the body using low intensity ultrasound and then released by destroying the microbubbles with high intensity ultrasound at a target site such as a tumour. Targeting species can also be attached to the surface of individual microbubbles to enable them to bind to specific receptors[3]. By localizing the treatment in this way, the risk of harmful side effects can be substantially reduced.

The response of a microbubble to ultrasound excitation depends on a combination of factors relating both to the microbubble itself and its environment. These include: the size of the microbubble, the nature of any surface coating, the frequency and pressure amplitude of the ultrasound field, the type and duration of exposure, the location of the microbubble and the concentration and properties of any neighbouring bubbles within that region. In order to develop effective protocols for ultrasound imaging and therapy it is important to understand the relative significance of each of these factors and to predict their effect upon microbubble behaviour. The work described in this paper is part of an ongoing project to develop appropriate theoretical models in conjunction with experimental studies[4] of microbubble dynamics. This paper will focus specifically on the influence of the microbubble coating upon the response of both single microbubbles and microbubble suspensions.

## 2 SINGLE MICROBUBBLES: EFFECT OF ENCAPSULATION

### 2.1 Equation of Motion for Spherically Symmetric Oscillations

The radial oscillations of an uncoated gas bubble can be described by the well known Rayleigh-Plesset equation[5]. If this equation is rederived for a bubble encapsulated by a thin surface coating it may be written as:

$$\rho_L\left(R\ddot{R}+\frac{3}{2}\dot{R}^2\right)+p_o-p_A-p_G(R)+\frac{4\dot{R}}{R}\mu_L=f_{ce}+f_{cd} \tag{1}$$

where $R$ is the instantaneous radius of the bubble, $R_o$ is its initial value, $\dot{R}$ and $\ddot{R}$ are the velocity and acceleration of the bubble wall respectively, $\rho_L$ is the density and $\mu_L$ the viscosity of the surrounding fluid, $p_o$ is the ambient pressure, $p_A$ is the pressure due to the applied sound field and $p_G$ is the pressure of the gas inside the bubble which was assumed to behave isothermally i.e.

$$p_G=\left(p_o+\frac{2\sigma_o}{R_o}\right)\left(\frac{R_o}{R}\right)^3 \tag{2}$$

The terms on the right hand side of the equation, $f_{ce}$ and $f_{cd}$, describe the additional elastic and dissipative resistance due to the surface coating. The form of these two terms depends on the nature of the coating being considered, e.g. whether it is a solid polymer or a surfactant monolayer. For the latter, $f_{ce}$ and $f_{cd}$ may be written as:

$$f_{ce} = -\frac{2}{R}\left(\sigma_o + \frac{K\Gamma_o^{x+1}}{(x+1)}\left(1-\left(\frac{R_o}{R}\right)^{2(x+1)}\right)\right) \tag{3}$$

$$f_{cd} = -\frac{4\dot{R}}{R^2}\eta_{so}e^{\frac{ZR_x^2}{\left(R^2-R_x^2\right)}} \tag{4}$$

where $\sigma_o$ is the equilibrium interfacial tension at $R = R_o$, $\Gamma_o$ is the initial concentration of surfactant on the bubble surface, $x$, $K$, $\eta_{so}$ and $Z$ are constants for a particular surfactant and $R_x$ is the limiting bubble radius beneath which the surface buckles* and the interfacial tension is reduced to zero. The derivation of these terms may be found in reference [6].

For a coating whose thickness is more than 1% of the initial bubble radius, an equation similar to equation (1) may be derived[7], but in this case the inertia term ($\rho_L\left(R\ddot{R}+1.5\dot{R}^2\right)$) will also contain a contribution from the coating, although this will be small in magnitude compared with that due to the surrounding liquid. For the purposes of this study, a thin surfactant shell will be considered, since this is the most appropriate model for the bubbles investigated in the associated experimental work[4]

The pressure field radiated by the bubble may be predicted using potential flow theory[8] as

$$p_{rad}(r) = \rho_L\left(\frac{1}{r}\left(R^2\ddot{R}+2R\dot{R}^2\right)-\frac{R^4\dot{R}^2}{2r^4}\right)+\left(p_o - p_A\right) \tag{5}$$

The parameter values used for the simulations were as follows: $R_o$ = 2.5 µm, $p_o$ = 0.1 MPa, $\sigma_o$ = 0.05 N m$^{-1}$ for a coated or 0.07 N m$^{-1}$ for an uncoated bubble, $\Gamma_o$ = 2 x 10$^{17}$ m$^{-2}$, $x$ = 0 unless otherwise specified, $K$ = 5.0 x 10$^{-18}$ N m, $\rho_L$ = 1000 kg m$^{-3}$, $\mu_L$ = 0.0015 Pa s, $\eta_{so}$ = 5 x 10$^{-8}$ N s m$^{-1}$, $Z$ = 0, $R_x = 0.8R_o$, 5 kPa < $p_A$ < 500 kPa and 1 MHz < $f$ < 3 MHz as specified for particular examples.

## 2.2 Pressure Dependent Behaviour

### 2.2.1 Comparison with an Unencapsulated Bubble

By setting $f_{ce} = 2\sigma_o/R$, equation (1) reduces to the Rayleigh-Plesset equation for an unencapsulated bubble which can be solved numerically[9] to predict the bubble's response. As shown in Figure 1a, for a 2.5 µm radius bubble excited at its natural frequency (1.24 MHz), the non-linear character of this response becomes increasingly pronounced with increasing amplitude of oscillation. Figure 1b demonstrates the significance of this effect in terms of the frequency content of the radiated field (equation 5). The green curves in Figures 1a and 1b indicate the effect of encapsulation on the microbubble response. Firstly, the resonance frequency is increased compared with the unencapsulated bubble, due to the additional elastic resistance provided by the coating ($f_{ce}$). Secondly, the amplitude of oscillation is diminished and, thirdly, the non-linear character of the oscillations is reduced so that the frequency spectrum of the radiated pressure contains fewer harmonic components.

* It should be noted that "buckling" in this sense refers to the arrangement of the phospholipid molecules rather than macroscopic folding of the membrane, although this may also occur.

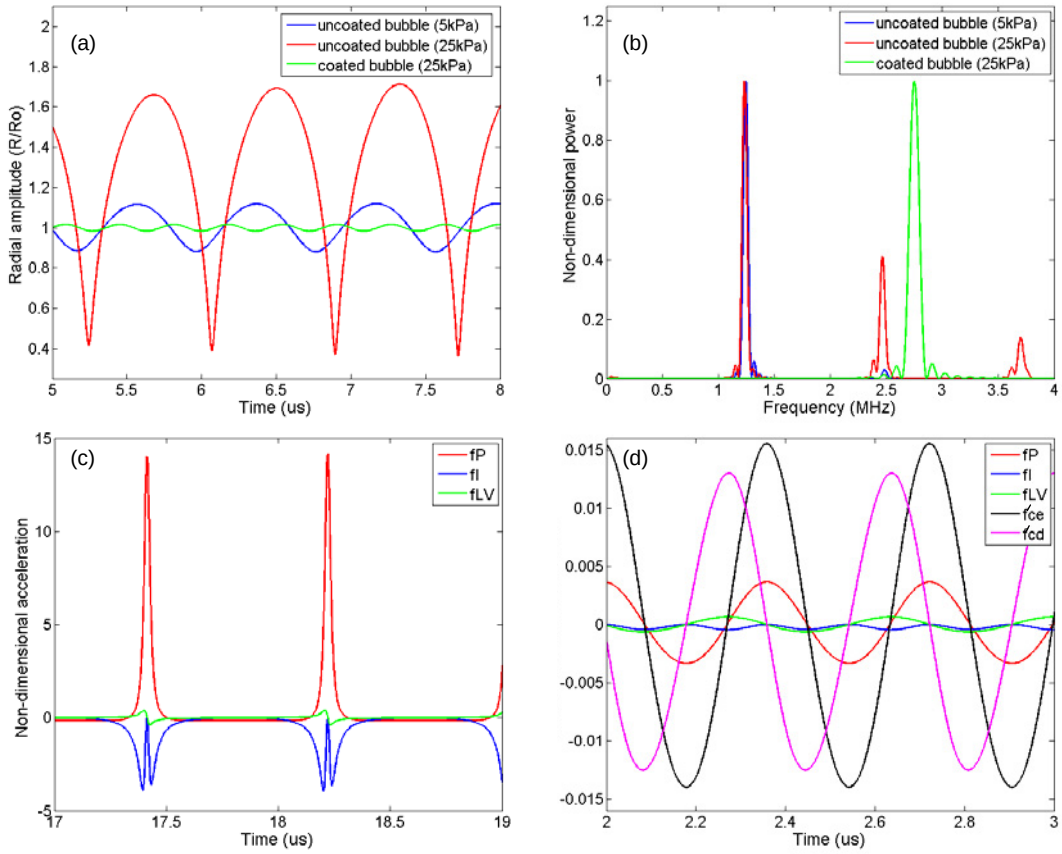


Figure 1. (a) Steady state radius-time curves for coated and uncoated air bubbles with initial radii 2.5 µm excited sinusoidally at their natural frequencies (2.75 MHz and 1.24 MHz respectively) at different pressure amplitudes. (b) Frequency spectra corresponding to the radiated pressure field from the bubbles shown in (a); signal power is shown normalised with respect to the maximum value for each bubble. Steady state acceleration components for (c) the coated and (d) the uncoated bubbles in (a) for an excitation pressure of 25 kPa.

A further effect of encapsulation may be observed as the excitation pressure is increased. For a given initial radius and excitation frequency there will be a negative pressure amplitude beyond which an unencapsulated bubble will undergo rapid collapse, dominated by the inertia of the surrounding fluid. This is indicated in Figure 1d which compares the components of the acceleration of the bubble wall:

$$f_I = \frac{3}{2}\frac{\dot{R}^2}{R}\,,\; f_P = \frac{p_o - p_G}{\rho_L R},\; f_{LV} = \frac{4\mu_L \dot{R}}{\rho_L R^2} \qquad \text{(6 a,b,c)}$$

where the subscripts *I*, *P* and *LV* refer to inertia, pressure and liquid viscosity respectively. In contrast, the response of the coated bubble is dominated by the coating (components $f'_{ce}$ and $f'_{cd}$ in Figure 1c where ' denotes division by $R\rho_L$) until a much higher negative pressure threshold is reached. This is an important consideration for assessing the potential of microbubbles to cause harmful bio-effects as these are believe to be associated with inertial collapse[10]. Encapsulation also changes the relationship between the bubble resonance frequency (i.e. the frequency at which the amplitude of oscillation is maximised) and the excitation pressure.

### 2.2.2 Non-linearity of the Encapsulating Material

Although, as above, the encapsulating material has a constraining effect upon the microbubble oscillations, it also introduces an additional source of non-linear behaviour. As shown in equation (3), the interfacial tension at the bubble surface depends upon the concentration of surfactant molecules there and hence varies as the bubble expands and contracts. This is analogous to a material having a strain dependent shear modulus. Similarly, as shown in equation (4), the effective viscosity of the coating may also be a non-linear parameter. Consequently, non-linear behaviour may be observed with coated bubbles even at very low excitation pressures, where an uncoated bubble would behave linearly. Some examples from experimental studies are described in [4], in particular, "compression- only" behaviour[11] of surfactant coated bubbles, which is illustrated in Figure 2a. Figure 2b shows the corresponding frequency spectrum for the radiated pressure from bubbles having linear and non-linear coatings ($x$ = 0 and $x$ = 0.2 respectively in equation (3)). This additional non-linearity may potentially be exploited in improving contrast agent detection, particularly since it reduces the need for elevated excitation pressures, although it can also be undesirable if the frequency content of the scattered field from a microbubble suspension is used to deduce e.g. the bubble size distribution.

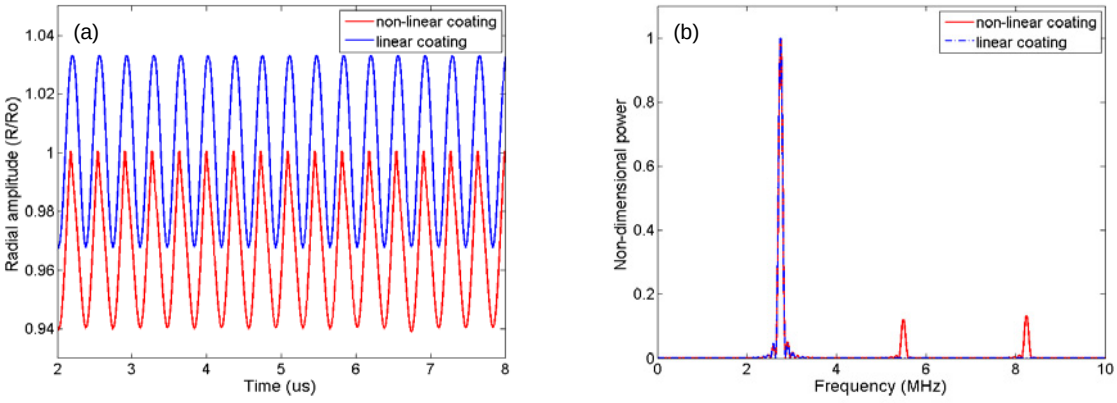


Figure 2. (a) Steady state radius-time curves for air microbubbles with initial radii 2.5 µm with linear and non-linear coatings (exponent in equation (3) $x$ = 0 and $x$ = 0.2 respectively) excited sinusoidally at 2.75 MHz and 50 kPa pressure amplitude. (b) Frequency spectra corresponding to the radiated pressure field from the bubbles shown in (a).

Surface oscillations represent a further potential source of non-linearity[12] and again the presence of a coating on the bubble surface may have a number of different effects. It will inevitably increase resistance to the initiation of surface instabilities compared with an uncoated bubble. On the other hand, inhomogeneities in the coating may themselves generate surface oscillations. It is not clear to what extent these surface modes contribute to the radiated field, however, particularly for coated bubbles in the 1-10 µm size range and consequently their significance for diagnostic and therapeutic applications requires further investigation. The presence of a coating will also reduce the tendency of the bubble to undergo non-spherical oscillations as a result of its proximity to e.g. other bubbles or a blood vessel wall, but this is outside the scope of the present discussion.

## 2.3 Time Dependent Behaviour

### 2.3.1 Diffusivity of the Encapsulating Material

As above, encapsulation stabilises the microbubble against both dissolution and coalescence, firstly by reducing the interfacial tension and secondly by inhibiting diffusion of the gas in to the surrounding liquid. This effect can be described mathematically by equating the rate of change of bubble mass with the rate of diffusion across the bubble surface, following the approach adopted by Epstein and Plesset[13] for uncoated bubbles. For a bubble having a surface coating described by

equation (4), so that the interfacial tension varies with surface concentration, the rate at which the bubble radius changes is predicted by:

$$\dot{R} = \frac{\kappa_s BT\left(c_{si} - c_{ssat}\right)}{M\sqrt{\pi\kappa_s t}\left(p_o + \frac{4\sigma_o}{3R} + \frac{4}{3}\frac{\Gamma_o^{x+1}}{(1+x)}\frac{K}{R}\left(x\left(\frac{R_o}{R}\right)^{2(1+x)} + 1\right)\right)}\left\{1 + 2\sum_{n=1}^{\infty}\alpha^n e^{\frac{-n^2 l^2}{\kappa_s t}}\right\} \qquad (7)$$

where $\kappa_s$ is the diffusivity of the gas in the surfactant layer, $B$ is the universal gas content, $T$ is the absolute temperature, $c_{si}$ is the initial concentration of gas in the surfactant layer, $c_{ssat}$ is the saturation concentration of gas in the surfactant layer, $\alpha$ is the ratio of diffusivities in the surfactant layer and surrounding liquid, $n$ is the summation index, $l$ is the coating thickness, $t$ is time and $M$ is the molecular weight of the gas.

Figure 3a shows how the radius of an air bubble in water would be expected to change with time under constant ambient pressure, with and without a surfactant coating. Equation (7) neglects the effects of convective diffusion and in order to include this and the influence of a time varying pressure, such as sound field, the mass-transfer equations used to derive equation (7) must be coupled to equation (1). This has been done by Fyrillas and Szeri[14] for unencapsulated bubbles and bubbles in solutions containing surfactants. As shown in the next section, however, the applicability of the results to contrast agent microbubbles is limited on account of the fact that the quantities $\kappa_s$, $c_{ssat}$ and $\Gamma_o$ are themselves functions of time.

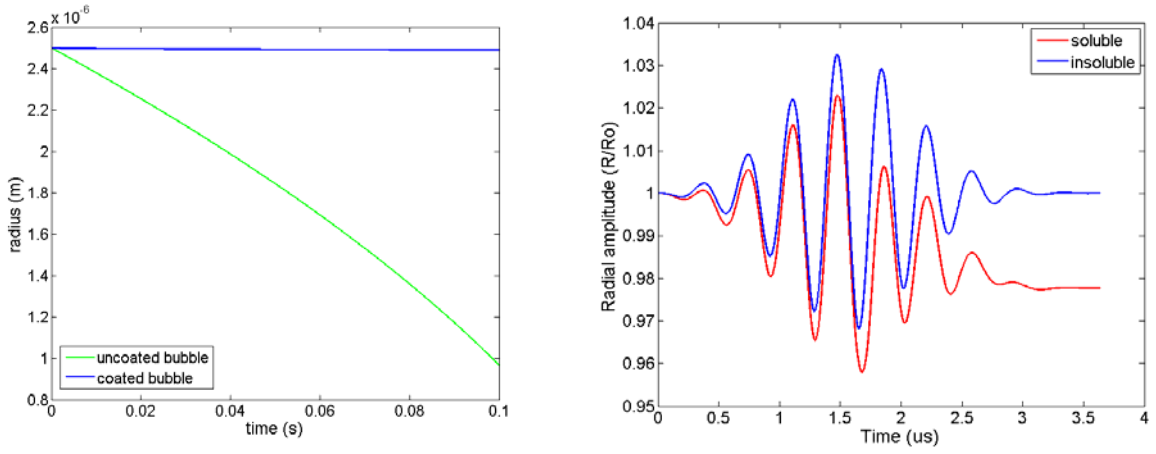


Figure 3. (a) Radius-time curves for coated and uncoated air bubbles with initial radii 2.5 µm under constant ambient pressure ($p_o$ = 0.1 MPa). (b) Radius-time curves for air microbubbles with initial radii 2.5 µm having soluble and insoluble coatings, excited with an 8 cycle Gaussian pulse, centre frequency 2.75 MHz, peak negative pressure 50 kPa.

### 2.3.2 Solubility of the Encapsulating Material

Experimental results[4,15] indicate that not only the gas content, but also the nature of the coating may vary with time, even over the course of a single ultrasound pulse. This may be due to rupture of the coating material, in the case of a polymer encapsulated bubble, or to a change in surfactant concentration at the bubble surface due to dissolution or lipid shedding. In order to describe the effect on the bubble oscillations fully therefore, the equation of motion for the bubble must be solved in conjunction with the mass transfer equations for both the gas and the coating material. Unfortunately, the latter are as yet poorly determined for the materials and frequencies relevant to contrast agent microbubbles. An approximate solution for the effect of coating dissolution can be obtained, however, by replacing the surface tension and surface concentration terms ($\sigma_o$ and $\Gamma_o$) in equation (4) by an exponential function $e^{\pm\pi t}$ where the time constant, $\tau$, is determined from empirical data for the solubility of the surfactant[16]. The results for a bubble excited by a single pulse are shown in Figure 3b.

# 3 MICROBUBBLE SUSPENSIONS

## 3.1 Effect of Microbubble Size Distribution

It is the behaviour of a microbubble suspension rather than that of individual microbubbles which is of most importance for clinical applications. Clearly, however, this will be strongly influenced by changes in the response of individual bubbles due to the effects discussed above. For example, the red and blue curves in Figure 4a show how the attenuation coefficient, $A$, for a suspension of surfactant coated microbubbles changes with the size distribution of bubbles present, where $A$ is found from the imaginary component of the effective wave number for the suspension[17]:

$$K_{eff}^2 = k_L^2 + 4\pi Nh \tag{8}$$

where $k_L$ is the wave number of surrounding liquid, $N$ describes the size distribution of the suspension and $h$ is the linear scattering function (which is an integral term for polydisperse suspensions). Variations in the size distribution may be due to differences in the composition of the initial suspension and/or to time dependent effects, as described above, and can have a significant effect upon the population response. This, in turn, may lead to inaccuracies in the interpretation of microbubble signals, particularly if these are to be used quantitatively, e.g. for perfusion measurements. Similar effects may arise as a result of variations in the characteristics of the microbubble coating as indicated by the green curve in Figure 4a which demonstrates the effect of increasing coating stiffness.

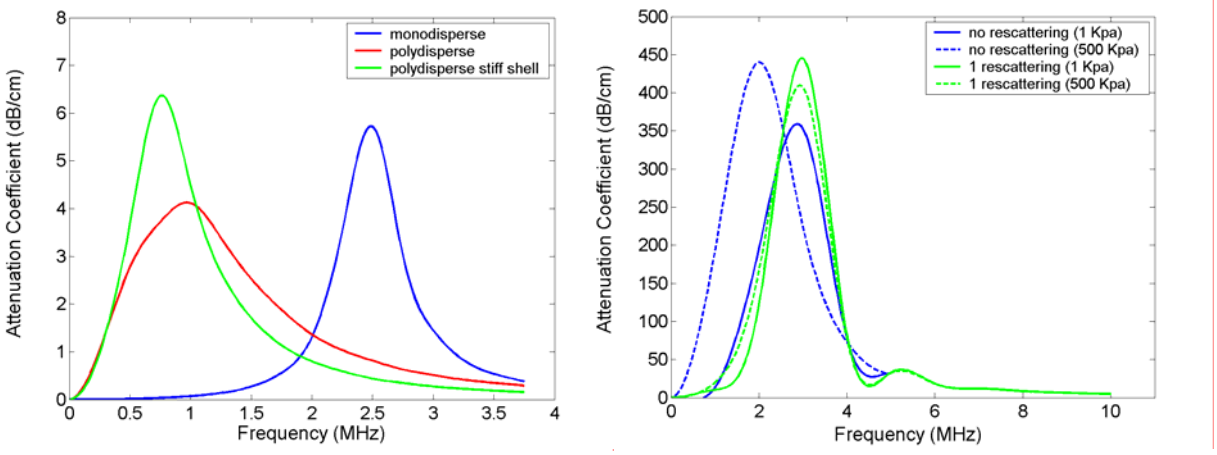


Figure 4. Variation in the attenuation coefficient for a coated microbubble suspension. (a) The effect of size distribution and coating stiffness. (b) The effect of rescattering and excitation pressure. In each case the mean bubble radius is 2.5 µm and the suspensions in (b) are monodisperse. The concentration in (a) and (b) is $10^4$ and $10^6$bubbles/ml respectively.

## 3.2 Effect of Microbubble Concentration

It is not only the response of individual bubbles which determines the properties of the suspension however, but also interactions between them, specifically dynamic coupling and multiple scattering of the sound field. The significance of these interactions depends upon the suspension concentration and whether or not a large proportion of the bubbles are excited at their resonance frequency, being negligible at low microbubble concentrations and/or far away from resonance. The solid curves in Figure 4b show how the attenuation through a bubble suspension varies with frequency at low excitation pressures with and without rescattering. As may be seen, attenuation may be substantially increased at resonance due to rescattering. The dashed curves indicate the effect of increasing insonation pressure upon the attenuation curves, showing that rescattering not only affects the magnitude of the attenuation coefficient but also the frequency at which it is maximised. Details of the solution of equation (8) for non-linear behaviour are given in [16]. Again, it is important that these effects are taken into account in image processing algorithms to avoid the formation of quantification errors and image artefacts. This will be discussed in more detail in [18].

# 4 REFERENCES

1. C. Harvey, J. Pilcher, R. Eckersley et al. Advances in ultrasound. Clinical Radiology 57, 157-177. (2002).
2. E. Unger, E. Hersh, M. Vannan et al. Local drug and gene delivery through microbubbles, Progress in Cardiovascular Diseases 44, 45-54. (2001).
3. A. Klibanov. Targeted delivery of gas-filled microspheres, contrast agent for ultrasound imaging, Advanced Drug Delivery Reviews 37, 139-157. (1999).
4. R. Eckersley, E. Stride and M. Tang. Microbubble contrast agents for medical ultrasound imaging: current issues and new directions. Proc. Inst. Acoustics Spring Conf. (2008)
5. M. Plesset and A. Prosperetti. Bubble dynamics and cavitation, Annu. Rev. Fluid Mech. 9, 145–185. (1977).
6. E. Stride. The influence of surface adsorption on bubble dynamics. Phil. Trans. Roy. Soc. A. (*in press*).
7. C. Church. The effects of an elastic solid surface layer on the radial pulsations of gas bubbles, J. Acoust. Soc. Am. 97, 1510-1520. (1995).
8. K. Vokurka. Amplitudes of free bubble oscillations in liquids. J. Sound and Vibration. 141, 259-275. (1990).

9. Simulations were performed using a Runge-Kutta solution (function ode45) in Matlab® (The Mathworks, Natick, MA, USA). (2006).
10. W. Nyborg. Biological Effects of Ultrasound: Development of Safety Guidelines. Part II: General Review. Ultrasound in Med. Biol 27, 301-333. (2001).
11. N. de Jong, M. Emmer, C. Chin et al. Compression only behaviour or phospholipid coated contrast bubbles, Ultrasound in Med. Biol. 33, 653-656. (2007).
12. M. Longuet-Higgins. Monopole emission of sound by asymmetric bubble oscillations, J. Fluid Mech. 201, 525-541. (1989).
13. P. Epstein and M. Plesset. On the stability of gas bubbles in liquid-gas solutions. J. Chem. Phys. 18, 1505-1509. (1950).
14. M. Fyrillas and A. Szeri. Dissolution or growth of soluble spherical oscillating bubbles, J. Fluid. Mech. 289, 295-314. (1995).
15. M. Borden, P. Dayton, S. Zhao and K. Ferrara. Physico-chemical properties of the microbubble lipid shell, Proc. IEEE Ultrasonics Symposium, 20-23 (2004).
16. R. Glazman. Damping of bubble oscillations induced by transport of surfactants between the adsorbed film and the bulk solution. J. Acoust. Soc. Am. 76, 890-896. (1984).
17. E. Stride and N. Saffari. Investigating the significance of multiple scattering in ultrasound contrast agent particle populations. IEEE Trans. Ultras. Ferr. Freq. Cont. 52, 2332-2345 (2005).
18 . M. Tang, R. Eckersley and E. Stride. Towards quantitative ultrasound imaging with microbubble contrast agents. Proc. Inst. Acoustics Spring Conf. (2008)